Stability of Cobalt Ferrite Colloidal Particles. Effect of pH and Applied Magnetic Fields

J. de Vicente, A. V. Delgado, R. C. Plaza, J. D. G. Durán, and F. González-Caballero*

Departamento de Física Aplicada, Facultad de Ciencias, Universidad de Granada, 18071-Granada, Spain

Received March 7, 2000. In Final Form: June 21, 2000

An experimental investigation is described on the stability of cobalt ferrite colloidal spheres, by analyzing the time variation of the optical absorbance of the suspensions as a function of pH and magnetic field strength. Structural and chemical analysis of the particles suggest that they are composed of a mixed cobalt−iron ferrite and magnetite, with some excess oxygen, probably coming from adsorbed water. In order to consider all posible particle−particle interactions that might be responsible for the observed behavior, the classical DLVO theory was extended to include magnetic dipole attractions. The electric double layer of the particles was characterized by electrophoresis, and it was found that the ferrite colloids have an isoelectric point (pH_{iep}, or pH of zero zeta potential, ζ) of ≅6.5. This is confirmed by stability measurements: the absolute value of the initial slope of the absorbance−time curves shows a pronounced maximum around pH 7. Concerning the effect of a uniform magnetic field (applied in the direction of the gravitational field), the most significant feature found was that above ≅1 mT, and for particle concentrations larger than ≅0.7 g/L, the suspensions appear more stable the stronger the applied field. Potential energy calculations, while explaining the lower stability of the suspensions around pH_{iep}, show that increasing magnetic fields decrease indeed the potential barrier between the particles, but not enough to ensure irreversible aggregation. It is hence suggested that the observed stability behavior is due to a long-range structuration of the dispersed particles that form long chainlike aggregates extending almost to the whole volume of the suspension. This may explain that the optical absorbance takes a longer time to decrease in the presence of a magnetic field applied in vertical direction, and also that the final fall in turbidity occurs at a faster rate than in the absence of the field.

1. Introduction

Colloidal particles are increasingly finding their way into many different fields of technology.[1−3] One of such fields is the preparation of ceramic magnets starting from concentrated slurries of ceramic particles in the colloidal range. However, because of the existence of strong magnetic interactions between magnetized particles, such interactions may considerably affect both the rheology[4−6] and the colloidal stability[7−9] of the suspensions. In fact, a rich variety of physical phenomena have been reported for the disperse systems that are known as magnetic fluids in a wide sense, including suspensions of permanent magnets (ferrofluids or magnetic fluids) or of magnetizable particles (magnetorheological fluids). In this work, we will focus on the tendency of the latter to aggregate either reversibly or irreversibly in the presence and in the absence of a magnetic field. Since the formation of aggregates can affect both the light scattering and sedimentation rate of the suspensions, our investigation has dealt with the time evolution of the turbidity of the systems, as a measure of the changes in both properties.

With the aim of making this study as quantitative as possible, we decided to use magnetic particles with spherical shape and narrow size distribution. The works of Matijević have demonstrated that this can be achieved for many different inorganic materials, and also magnetic ones.[10−12] In the present contribution, cobalt ferrite particles will be used as the object of the study; in addition to their intrinsic physical interest, they have been proposed as substitutes of magnetite whenever high electrical resistivity might be required, together with a response to applied magnetic fields.[13] Further, these ferrimagnetic particles can be prepared with the criteria mentioned above concerning homogeneity in both size and shape.[12]

Our aim in this work is to experimentally determine the stability of the ferrite particles in suspension and to find an explanation for the observed behavior in terms of the calculation of the total interaction energy between the particles. The latter will include not only the magnetic contribution but also electrical and van der Waals interactions. The study will thus require to characterize not only the magnetic moment of the particles but also their surface potential. The effects of pH and magnetic field on both the experimental determinations and the calculations of interaction energies will be described and discussed.

* Corresponding author. Fax: +34-958-243214. E-mail: fgonzale@ugr.es.

(1) Williams, R. A. *Colloid and Surface Engineering: Applications in the Process Industries*; Butterworth-Heinemann Ltd.: Oxford, UK, 1992.
(2) McKay, R. *Technological Applications of Dispersions*; Marcel Dekker: New York, 1994.
(3) Pugh, R.; Bergström, L. *Surface and Colloid Chemistry in Advanced Ceramics Processing*; Marcel Dekker: New York, 1994.
(4) Tang, X.; Conrad, H. *J. Rheol.* **1996**, *40*, 6.
(5) Volkova, O.; Cutillas, S.; Bossis, G. *Phys. Rev. Lett.* **1999**, *82*, 233.
(6) Felt, D. W.; Hagenbüchle, M.; Liu, J.; Richard, J. *J. Intelligent Mater. Sys. Str.* **1996**, *7*, 589.
(7) Tombácz, E.; Ma, C.; Busch, K. W.; Busch, M. A. *Colloid Polym. Sci.* **1991**, *269*, 278.
(8) Janssen, J. J. M.; Baltussen, J. J. M.; van Gelder, A. P.; Perenboom, J. A. A. J. *J. Phys. D: Appl. Phys.* **1990**, *23*, 1455.
(9) Wang, H.; Wen, C. S. *J. Colloid Interface Sci.* **1999**, *213*, 606.
(10) Matijević, E. *Annu. Rev. Mater. Sci.* **1985**, *15*, 483.
(11) Sugimoto, T.; Matijević, E. *J. Colloid Interface Sci.* 1980, *74*, 227.
(12) Tamura, H.; Matijević, E. *J. Colloid Interface Sci.* 1982, *90*, 100.
(13) Geoffroy, O.; Porteseil, J. L. In *Magnétisme*; Trémolet de Lacheisserie E., Ed.; Presses Universitaires de Grenoble: Grenoble, France, 1999.

10.1021/la0003490 CCC: $19.00
Published on Web 09/13/2000

2. Experimental Section

2.1. Materials. All chemicals used were purchased from either Merck (Germany) or Panreac (Spain) with analytical quality and were not further purified. Water used in the preparation of the solutions and suspensions was of Milli-Q quality (Milli-Q Academic, Millipore, France).

2.2. Methods. *Particle Preparation.* Ferrite particles were prepared following the coprecipitation method described by Tamura and Matijević.[12] The method involves the coprecipitation of iron(II) and cobalt(II) hydroxides that, upon heating at 90 °C in an oxidizing aqueous medium, yield the ferrite particles. The first stage of the synthesis is the preparation of an aqueous solution containing 1.25×10^{-1} M $FeSO_4 \cdot 7H_2O$, 7.5×10^{-2} M $Co(NO_3)_2 \cdot 6H_2O$, 0.2 M KNO_3, and 0.1 M KOH. Water was previously purged with pure N_2 for at least 30 min to avoid the presence of dissolved oxygen as much as possible. This is needed to prevent the oxidation of ferrous ions to ferric ones prior to the necessary formation of ferrous hydroxide. Not only was water purged with nitrogen, but this gas was also bubbled through the starting solution mentioned, in which KOH provides the hydroxyl ions required for the formation of the hydroxides, and NO_3^- ions from the dissolved KNO_3 will be responsible for the controlled oxidation of Fe^{2+} to Fe^{3+}, required for the obtention of the iron(III) oxide that is also present in the ferrite.

This starting solution is placed in 50 cm^3 stoppered test tubes. Each tube will contain 20 cm^3 of the mixture, and they are immersed in an oil bath (Memmert, Germany) preheated at 90 °C and kept at such temperature for 24 h. The suspensions thus obtained are repeatedly cleaned of undesired material (such as goethite, α-FeOOH) by magnetic sedimentation. Due to the not very hard hysteresis cycle of the particles (we will discuss this below), the separation of nonmagnetic particles can be achieved by placing the tubes between the poles of a permanent magnet ($B = 0.42$ T) and the material not adhered to the wall in contact with the pole is pipetted off, and substituted with water. The process is considered finished when the supernatant thus obtained is transparent and has low electric conductivity (<2 μS/cm). The geometrical characteristics of the particles were studied by transmission electron microscopy (Zeiss EM 902, Germany).

Chemical Composition. Both the bulk and surface chemical composition of the ferrite particles were determined. The former was achieved by atomic absorption spectroscopy (Perkin-Elmer 5100), whereas X-ray photoelectron spectroscopy (XPS, Perkin-Elmer, USA) was used as a tool for surface chemical analysis. The bulk structure of the material was analized by X-ray diffraction using the Debye−Scherrer method in a Philips PW1710 powder diffractometer (Netherlands).

Magnetic Properties. The magnetization, M, of the solids was measured as a function of the applied magnetic field, H, in a Manics DSM-8 magnetosusceptometer (France). The hysteresis of the magnetization was obtained by changing H between −19 000 and +19 000 Oe (−1512 and +1512 kA/m). These measurements were carried out at room temperature (293.0 ± 0.2 K).

Electrical Surface Characterization. The electrical state of the particle surface, for the different compositions (ionic strength and pH) of the dispersion medium, was ascertained by electrophoretic mobility measurements in a Malver Zetasizer 2000 electrophoresis equipment (Malvern Instruments, England).

Stability Determination. The stability of the suspensions was inferred from optical absorbance (or turbidity) measurements as a function of time. A Milton Roy Spectronic 601 (USA) spectrophotometer set at a wavelength of 550 nm was used. Square cuvettes with 1 cm light path were used; the center of the light beam strikes the cuvette 1.5 cm above its bottom. When the effect of the magnetic field was studied, a pair of Helmholtz coils (Phywe, Germany) were used; the center of the cuvette was located at the center of the line joining the centers of each coil. The magnetic field inside the sample could be varied between 0 and 2.5 mT and was measured with a Hall-effect teslameter (Phywe, Germany). Variations of the magnetic field inside the sample were always below 10%.

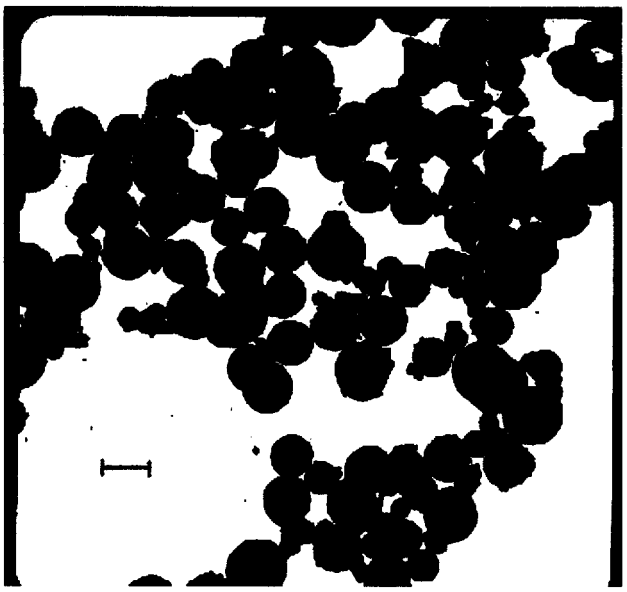

Figure 1. TEM picture of the cobalt ferrite spheres synthesized. Bar length: 1 μm.

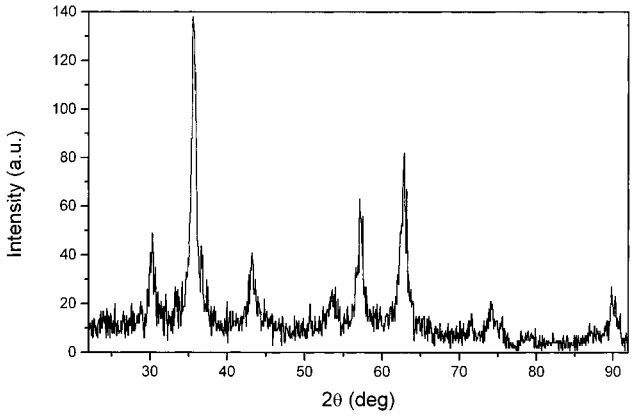

Figure 2. X-ray diffraction pattern of the cobalt ferrite particles.

3. Results and Discussion

3.1. Particle Morphology and Composition. TEM micrographs like those shown in Figure 1 demonstrate that spherical and quite monodisperse particles can be obtained with the method of Tamura and Matijević.[12] Measurements on 390 particles yielded an average diameter of 850 ± 150 nm.

Bulk chemical composition was obtained by atomic absorption, using the average of two samples. The mass percentages of the elements were 10.8% Co, 54.3% Fe, and 34.9% O; this composition corresponds to the empirical formula $CoFe_{5.3}O_{11.9}$. Since it is likely that in this synthesis magnetite is also produced, the empirical formula can be explained by assuming that the material obtained corresponds to $yCo_xFe(II)_{1-x}Fe(III)_2O_4 + zFe_3O_4 + 3.5O$, with $y + z = 2.1$. This oxygen excess must come from adsorbed water molecules, not totally eliminated in the mild drying process employed.[14]

X-ray diffraction data (Figure 2) suggests the coexistence in the sample of two crystal structures (note the shoulders that are visible in the main diffraction peaks), one of which corresponds closely to maghemite (γ-Fe_2O_3: the Fe^{2+} positions are unoccupied). The second structure could be due to the mixed ferrite.

(14) Sidhu, P. S.; Gilkes, R. J.; Posner, A. M. *J. Inorg. Nucl. Chem.* **1978**, *40*, 429.

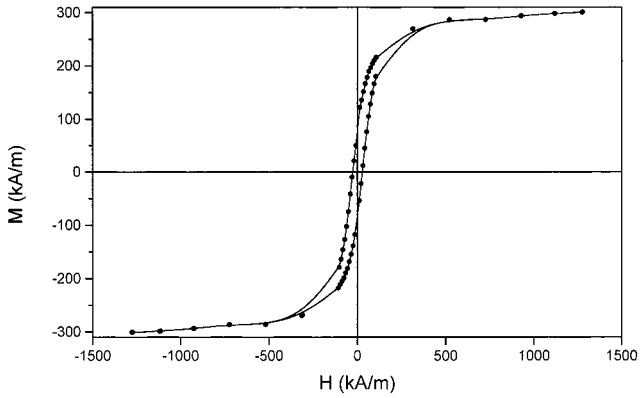

Figure 3. Hysteresis cycle of the magnetization of cobalt ferrite powder, at room temperature (293.0 ± 0.2 K).

The question now remains of whether the structure of the particles is homogeneous or rather there is an excess surface concentration of any of the metal ions. This possibility was explored by XPS data. The results obtained from XPS revealed that the mass percents of the elements were 3.43% Co, 31.74% Fe, and 64.83% O, which corresponds to the empirical formula $CoFe_{9.8}O_{69.6}$ The high oxygen content could be explained due to adsorption of water molecules on the surface.

3.2. Magnetic Properties. Figure 3 shows the hysteresis loop of the powder of synthetic spheres. As observed, a saturation magnetization M_s of 2.7×10^5 A/m is obtained; this value can be compared to experimental determinations[15] on pure $CoOFe_2O_3$, for which $M_s = 3.94 \times 10^5$ A/m.

Figure 3 demonstrates that the synthesized ferrite is a not very hard magnetic material, because of its small coercive field $H_c = 0.275 \times 10^5$ A/m (≅346 Oe) and its high saturation magnetization. Furthermore, its remanent magnetization of 0.82×10^5 A/m is quite low in comparison to that of hard magnetic materials.

3.3. Electrophoretic Mobility and Zeta Potential. In Figure 4 we show the zeta potential (deduced from the electrophoretic mobility, μ_e, using O'Brien and White's theory, see ref 16) of ferrite spheres, as a function of pH and in the presence of different $NaNO_3$ concentrations. Whatever the latter, all the curves show an isoelectric point (pH_{iep}) around pH = 6.5, a value that is in good agreement with previously reported data on these colloids.[12] In view of the data presented in Figure 4, it can be said that pH can be considered as the variable of interest for the electrical characterization of the cobalt ferrite surface.

3.4. Stability of the Suspensions. *Effect of pH and Ionic Strength*. All our inferences on the stability of cobalt ferrite particles will be based on the characteristics of the evolution with time of the optical absorbance (A) of the suspensions in the different conditions studied. Figure 5 is an example: it displays the absorbance of ferrite suspensions as a function of time for constant ionic strength and different pH values. All suspensions contained 2 g/L of particles and 10^{-3} M $NaNO_3$ suspensions. Because of the density and diameter of the particles, there is an overall trend of A to decrease with time, due to the disappearance of the solids from the illuminated region as settling proceeds. Nevertheless, this trend changes with pH, this being a clear indication of the different sedimentation velocities of the particles depending on their

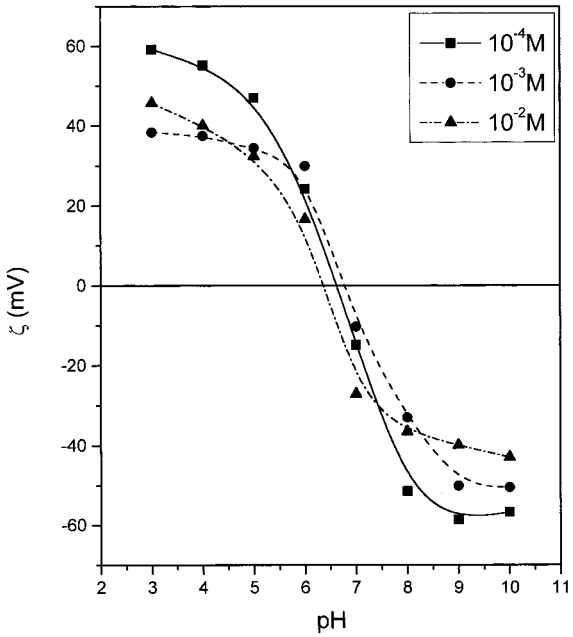

Figure 4. Zeta potential (ζ) of cobalt ferrite particles as a function of pH in different $NaNO_3$ concentrations.

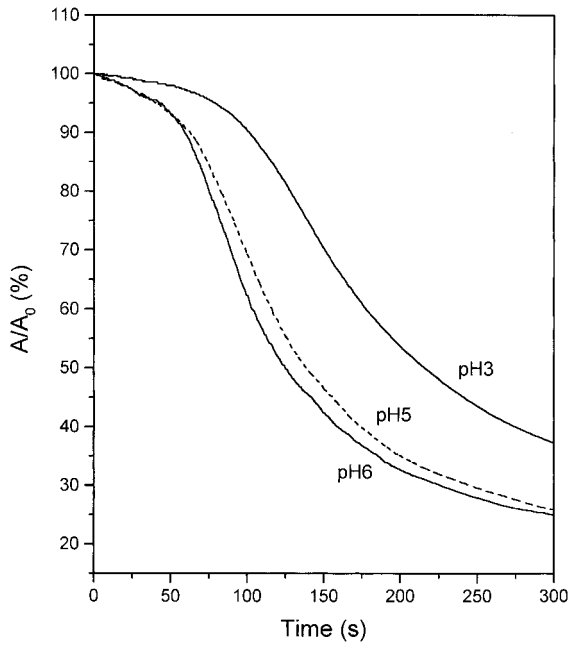

Figure 5. Optical absorbance A (expressed as % of initial absorbance, A_0) of cobalt ferrite particles as a function of time for different pH values. Ionic strength: 10^{-3} M $NaNO_3$.

state of aggregation. In particular, it is clearly observed that the absorbance decreases at a faster rate (mainly, at short times after the beginning of the experiment) when the pH is closer to the pH_{iep} of the particles.

The overall behavior is better appreciated if the initial slope of the A/A_0-t curves (A_0 is the suspension absorbance for $t = 0$) is plotted as a function of the quantity of interest. Thus, Figure 6 shows $[d(A/A_0)/dt]_{t=0}$ vs pH for two ionic strengths, namely, 10^{-3} and 10^{-2} M $NaNO_3$. It is clearly seen that, whatever the ionic strength, the suspension stability is most sensitive to pH: the sedimentation rate increases ($d(A/A_0)/dt$ decreases) as we approach pH = 7−7.5 from the acid side, and rapidly decreases as we get into the basic pH range. In other words, the suspensions are more stable the further their pH is from neutrality; this was to be expected in view of the data presented in

(15) Trémolet de Lacheisserie, E. *Magnétisme*; Presses Universitaires de Grenoble: Grenoble, France, 1999.

(16) O'Brien, R. W.; White, L. R. *J. Chem. Soc., Faraday Trans. 2* **1978**, *74*, 1607.

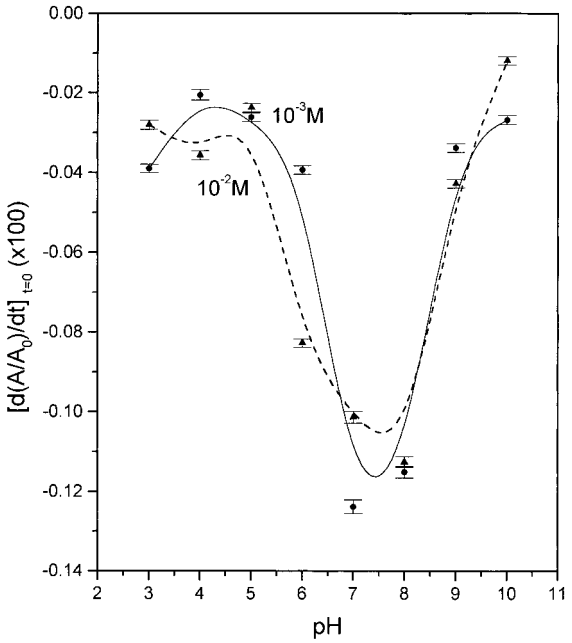

Figure 6. Initial slope of A/A_0-t plots for cobalt ferrite suspensions as a function of pH for different ionic strengths.

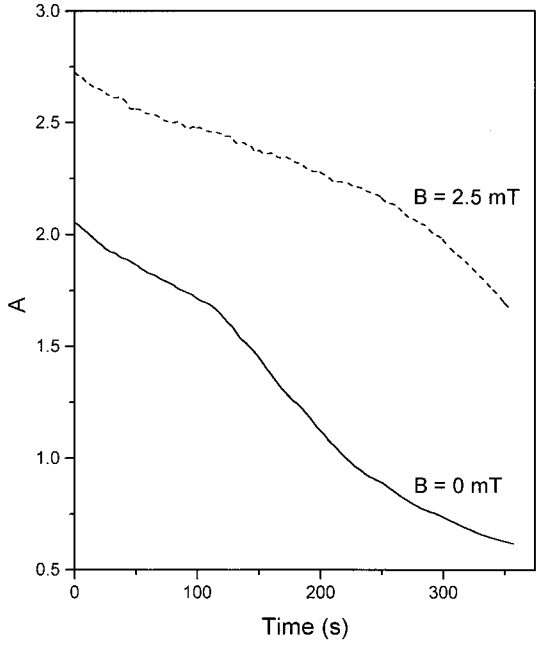

Figure 7. Absorbance of cobalt ferrite suspensions in water as a function of time with and without a constant field $B = 2.5$ mT parallel to the gravitational field.

Figure 4 and the fact that the zeta potential of the particles is zero in the vicinity of pH 7. Nevertheless, we will support this conclusion on interaction energy calculations below.

3.5. Effect of Applied Magnetic Fields. *Magnetic Field Strength.* From the magnetic character of the particles, a significant effect of a uniform applied magnetic field on the sedimentation rate of the particles was expected. Our first experiments were performed by allowing the particles settle with the field constantly applied: Figure 7 shows A versus time with and without a field (parallel to the gravitational field) of 2.5 mT. The suspensions had a particle concentration of 1 g/L without added electrolyte. The interesting result here is that the suspensions are clearly more stable in the presence of the field: the initial slope is smaller when B is applied. We

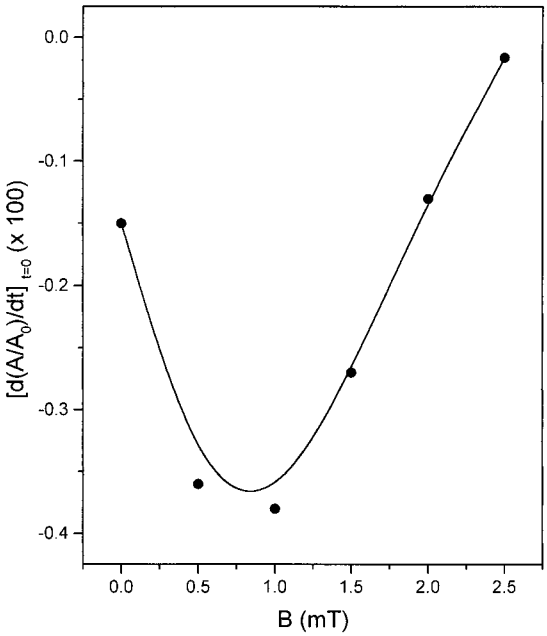

Figure 8. Initial slope of A/A_0 versus time for ferrite particles dispersed in water, as a function of magnetic field strength.

suggest that the field magnetizes the particles and that the subsequent attraction between the individual magnetic moments brings about the formation of large flocculi occupying most of the suspension volume. This explains the slow absorbance changes. After sufficiently long time, the flocculi break and sediment rapidly as they are formed by many particles. This might be the reason for the rapid fall in absorbance at longer times in the presence of B.

The experiments were repeated with different field strengths (applied in the vertical direction) as shown in Figure 8, where the initial absorbance slope is plotted vs B. It can be seen that the suspensions are more unstable as the field is increased from 0 to 1 mT; higher fields invert that trend and $[d(A/A_0)/dt]_{t=0}$ approaches zero for $B = 2.5$ mT. This behavior appears to be consistent with the explanation given to the results in Figure 7: the field induces magnetic moments in the particles, but only if B is high enough the magnetic attraction will be sufficiently strong to form large aggregates. At low B, the range of the interaction will be shorter, this giving rise to the formation of smaller aggregates that settle rapidly.

In order to confirm the hypothesis of formation of a long-range structure of the particles in the presence of the magnetic field, we took a series of pictures of the suspensions as a function of time. Figure 9 illustrates how significant the effect of B is on the sedimentation pattern: as observed, large aggregates remain in suspension in the presence of the field, for a time long enough for all particles to settle if no field is applied. The vertical orientation of the aggregates is not clearly seen in the pictures.

A thermodynamic study of this phenomenon has been described in ref 17, where it was shown that thermodynamic instability and breakdown of the suspension into separated phases can occur for certain values of both the applied field strength and particle concentration. In fact, in the region of instability, arbitrarily small fluctuations in concentration may grow to form large particle accumulations. This may be the process responsible for our stability data.

(17) Blums, E.; Cebers, A.; Maiorov, M. M. *Magnetic Fluids*, Walter de Gruyter & Co: Berlin, 1996.

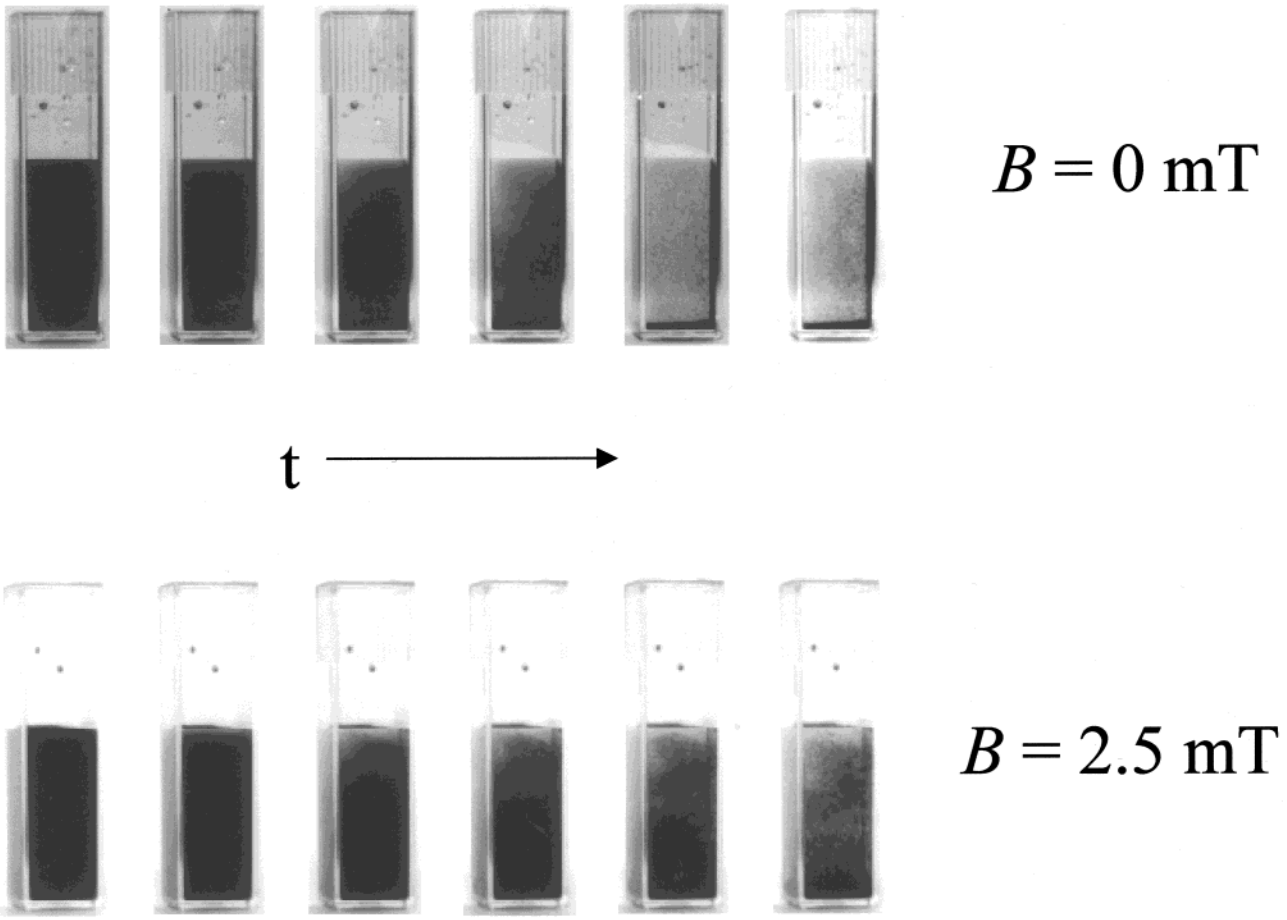

Figure 9. Snapshots of settling suspensions of ferrite spheres in water with (bottom) and without (up) application of a vertical magnetic field $B = 2.5$ mT. Time interval between the first and the last picture ≅3 min.

Particle Concentration. Given that both the absorbance and the number of pair interactions (both magnetic and nonmagnetic) between the particles depend on the concentration of solids, this was another interesting quantity to analyze. Thus, Figure 10 shows the absorbance as a function of time for suspensions of cobalt ferrite particles of different concentrations, with and without applied field (vertical $B = 2.5$ mT). Note that the initial absorbance, A_0, is roughly proportional to the concentration of solids, as expected. But it is also worth mentioning that A_0 is, for any concentration >0.5 g/L, larger when the field is applied. This is most likely due to the magnetic flocculation induced by the field: the extinction cross section of the complex aggregates formed must be larger than that of primary particles,[18] hence the larger absorbance measured in the presence of the magnetic field. For low particle concentrations, on the contrary, the situation is reversed, and A_0 is slightly lower for $B \neq 0$ than for $B = 0$: apparently, in the case of very low concentrations, interparticle distances are so large that dipole−dipole interactions do not produce flocculation. The initial slopes of the curves shown in Figure 10 are plotted as a function of particle concentration, c, in Figure 11. This graph demonstrates that the effect of the field on the stability is only appreciable for $c \geq 0.5$ g/L. For lower concentrations, the aggregates formed have a relatively small volume and simply settle as large particles. Only when the number of particles in suspension is sufficiently high can large aggregates, extending to most of the experimental volume, be formed.

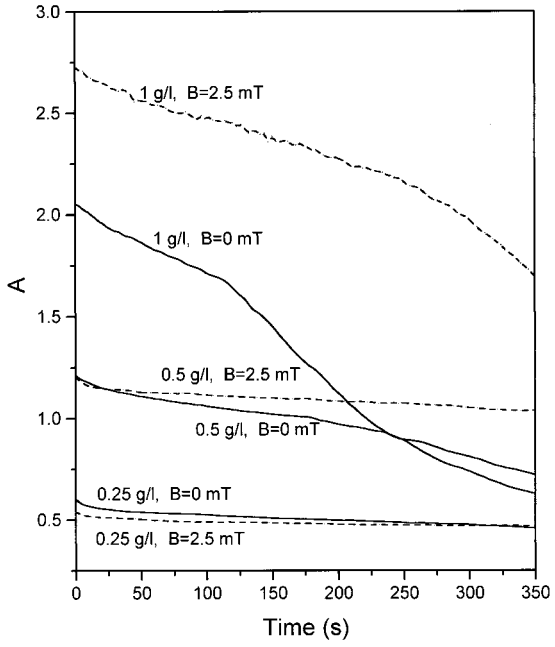

Figure 10. Absorbance of cobalt ferrite suspensions as a function of time with and without vertically applied magnetic field for the particle concentrations indicated. No added electrolite.

Effect of Magnetic Field Direction. Let us now consider how these arguments apply for a magnetic field applied horizontally. Figure 12 shows the time evolution of the absorbance of the suspensions of ferrite particles in water,

(18) Bijsterbosch, B. H. In *Solid/Liquid Dispersions*; Tadros, Th. F., Ed.; Academic Press: London, 1987; p 91.

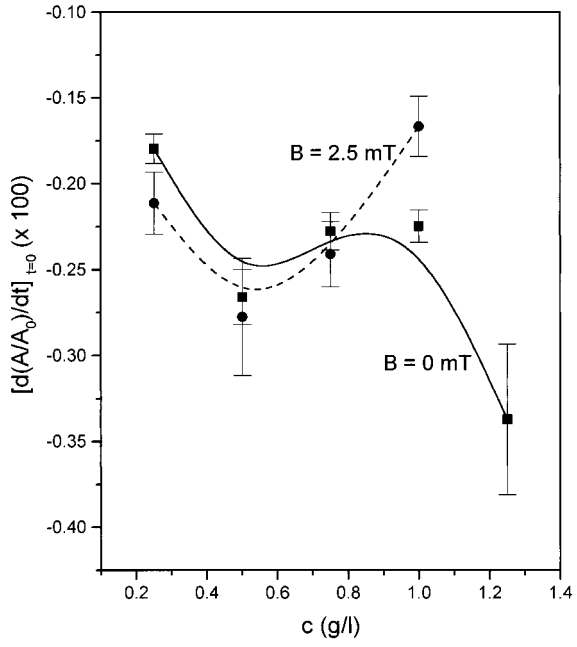

Figure 11. Initial slopes of the curves of Figure 10, normalized by the $t = 0$ absorbance in each case.

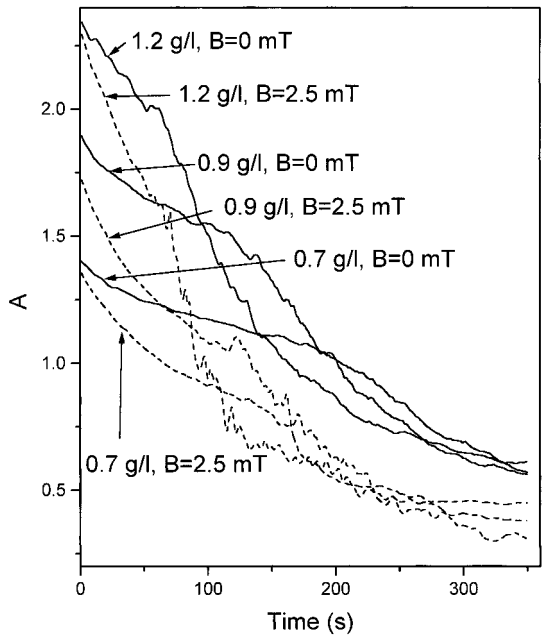

Figure 12. Same as Figure 10, but for a horizontally applied magnetic field.

for different particle concentrations (ranging between 0.7 and 1.2 g/L), with and without field. Two essential differences are found when these results are compared to those in Figure 10 (vertical field): the sedimentation of the particles is faster in the presence of the horizontal field, and, furthermore, no significant differences are observed between the initial absorbances measured with and without H. The reasoning given above, concerning the structuring effect of the magnetic field, can also be applied in this case. Thus, roughly horizontal particle chains will also form in horizontal fields, but it is unlikely that they extend between opposite walls of the cuvette. Hence they will sediment under gravity at a faster rate than in the absence of the horizontal field, and this will provoke a faster decay of absorbance with time when H is applied. Furthermore, the two opposite effects of enhanced sedimentation and aggregation may explain that

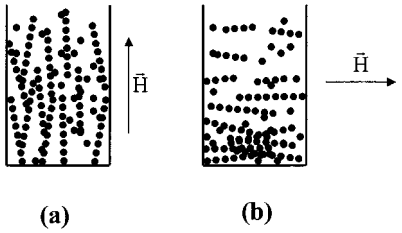

Figure 13. Schematic view of possible internal structures of the suspensions for vertical (a) and horizontal (b) magnetic fields.

the initial absorbance is similar for $H = 0$ and $H \neq 0$. Figure 13 illustrates, with a schematic picture, the possible internal structuration of the suspensions when a vertical (Figure 13a) or horizontal (Figure 13b) magnetic field is applied.

Interaction Energy between Particles. As mentioned above, the observed stability of the suspensions should be explained in terms of both magnetic and nonmagnetic interactions between them. The former can be expresed in terms of a potential energy function, V_M, given by[19]

$$V_M = -\frac{8\pi\mu_0 M^2 a^3}{9\left(\frac{s}{a}+2\right)^3} \quad (1)$$

where M is the magnetization of the material, a the radius of the particles, s the distance between the surfaces of two interacting particles, and μ_0 is the permeability of the vacuum. Equation 1 is obtained from the expression for the potential energy of interaction between two magnetic dipoles of strengths $\vec{m}_i$ ($i = 1, 2$) separated by a distance $\vec{r}$[19]

$$V_M = \frac{\mu_0}{4\pi}\left[\frac{\vec{m}_1\cdot\vec{m}_2}{r^3} - 3\frac{(\vec{m}_1\cdot\vec{r})(\vec{m}_2\cdot\vec{r})}{r^5}\right] \quad (2)$$

under the simplifying assumptions that both magnetic moments are parallel, of the same strength, and oriented head-to-tail. The common value of the magnetic moments was calculated from the magnetization multiplied by the particle volume. Since the experiments were performed at low magnetic fields, the magnetization will be considered proportional to H, using $\chi = 0.94$, as determined from experimental measurements.

The electrostatic repulsion between the electric double layers of the particles can be calculated from the following potential:[20]

$$V_{EL} = 2\pi\epsilon_r\epsilon_0 a\xi^2 \ln[1 + e^{-\kappa s}] \quad (3)$$

where it is assumed that the particle has a constant and moderate surface potential and that the diffuse layer potential can be identified with the electrokinetic or zeta potential, ζ. In eq 3, ϵ_r is the relative dielectric constant of the liquid, ϵ_0 is the permittivity of the vacuum, and κ is the reciprocal Debye length.

(19) Rosensweig, R. E. *Ferrohydrodynamics*; Cambridge University Press: Cambridge, UK, 1985.
(20) Hunter, R. J. *Foundations of Colloid Science*; Clarendon Press: Oxford, UK, 1987; Vol. I

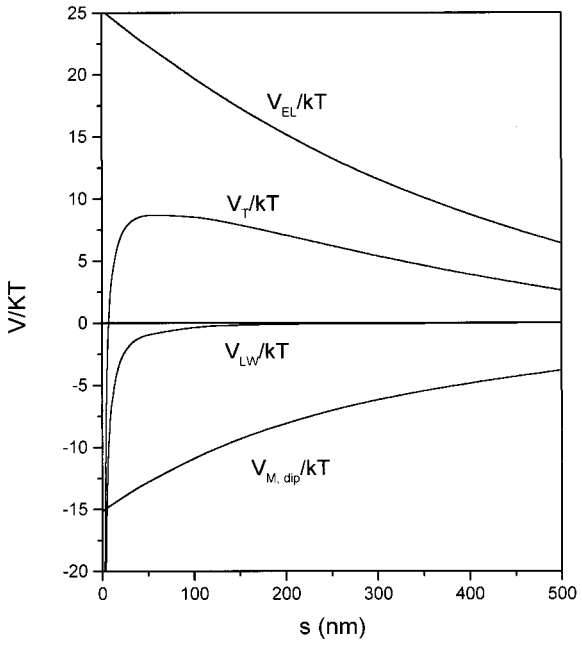

Figure 14. Potential energy of interaction between the ferrite spheres dispersed in water, as a function of distance between surfaces, *s*. V_{LW}, van der Waals; V_M, magnetic; V_{EL}, electric double layer; V_T, total energy.

Finally, the van der Waals atraction between the same spheres can be obtained from[21]

$$V_{LW} = \left(-\frac{A}{6}\right)\left[\frac{2a^2}{s(4a+s)} + \frac{2a^2}{(2a+s)^2} + \ln\frac{s(4a+s)}{(2a+s)^2}\right] \quad (4)$$

where A is the Hamaker constant, whose value was estimated to be 9×10^{-21} J, based on a thermodynamic study of the ferrite/solution interface.[22]

Figure 14 illustrates the dependence with distance of each of the three contributions (eqs 1, 3, and 4) to the total interaction energy, for particles suspended in water ($\zeta =$ 9 mV). As observed, the attractive magnetic interaction is stronger than van der Waals attraction, except at very short distances of approach, because of the finite value attained by V_M when $s = 0$. Figure 14 also indicates that, in spite of the superposition of V_M and V_{LW} attractions, the overall interaction, V_T, is dominated by electric double layer repulsions, explainable by the large double layer thickness of the particles dispersed in water.

Similar calculations were performed when the particles were dispersed in $NaNO_3$ solutions of different pH values. The results for the case of $[NaNO_3] = 10^{-2}$ M are displayed in Figure 15 (similar trends, not shown for brevity, were found for 10^{-3} M $NaNO_3$ solutions), for the case $B = 0$. As observed, the potential energy curves are in reasonable qualitative agreement with the turbidity data of Figures 5 and 6: as expected, the poorer stability of the suspensions close to the isoelectric point corresponds to the lowering of the potential barrier preventing particle aggregation. It is hence more interesting to consider the effect of applied magnetic fields on the interaction potential, as shown in Figure 16, for ferrite spheres dispersed in water. It can be seen that the application of increasing magnetic fields reduces the height of the potential energy barrier, thus favoring particle aggregation, in agreement with the results in Figures 7−12.

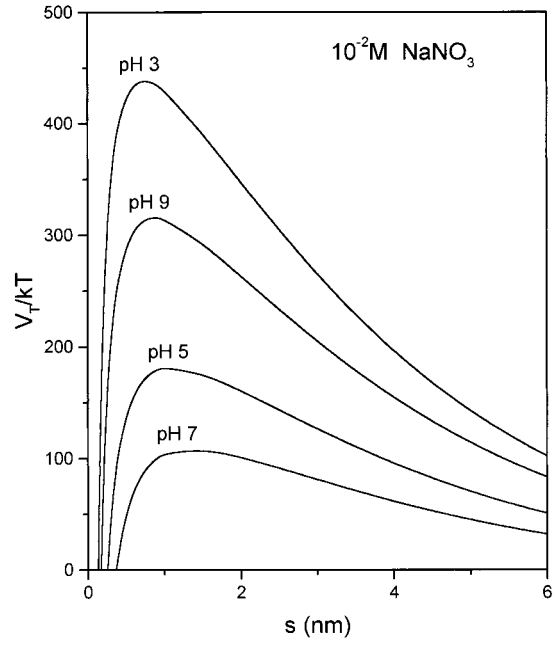

Figure 15. Interaction potential as a function of the distance *s* between ferrite particles, for different pH values and no applied magnetic field.

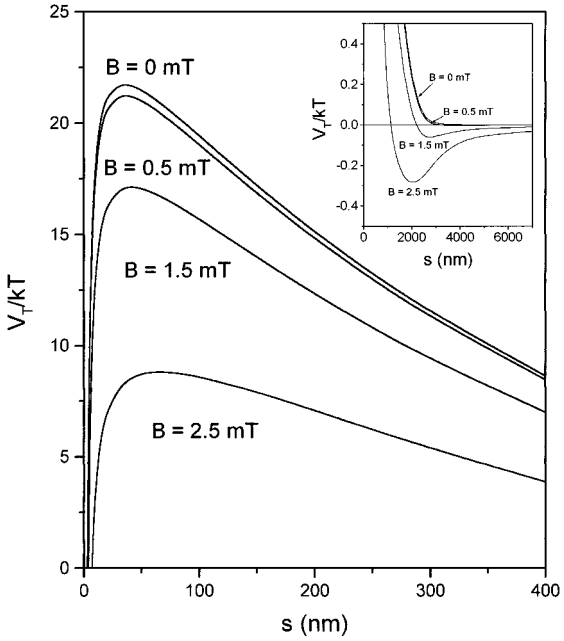

Figure 16. Total interaction potential between the ferrimagnetic colloidal particles in water as a function of distance for different applied magnetic fields. Inset: Detail of the long distance behavior of V_T.

Note that, in fact, the potential maximum is only $\cong 8kT$ for $B = 2.5$ mT. But most interestingly, the inset in Figure 16 shows that the application of fields above 0.5 mT brings about a shallow secondary minimum in the potential energy for long separations between the particles. This appears to be coherent with the settling behavior with increasing B shown in Figure 8, where as mentioned, it can be seen that a minimum field of about $\cong 1$ mT is needed to achieve structuration of the suspension. The fact that the secondary minimum is not deep might explain the

(21) Gregory, J. *J. Colloid Interface Sci.* **1966**, *22*, 342.
(22) de Vicente, J.; Durán, J. D. G.; González-Caballero, F.; Delgado, A. V., to be published.

observation that the suspensions are readily redispersed by mild shaking of the cuvette.

Acknowledgment. Financial support for this work by CICYT, Spain, under Project MAT 98-0940, and the assistance of Prof. D. Martín-Ramos in X-ray diffraction experiments are gratefully acknowledged.

LA0003490